Separation and Purification Technology 285 (2022) 120303

Contents lists available at ScienceDirect

Separation and Purification Technology

journal homepage: www.elsevier.com/locate/seppur

Catalytic selective recovery of silver from dilute aqueous solutions and e-waste leachates

Erez B. Ruck, Gidon Amikam, Yonatan Darom, Naama Manor-Korin, Youri Gendel *

Faculty of Civil and Environmental Engineering, Technion-Israel Institute of Technology, Haifa 32000, Israel

ARTICLE INFO

Keywords:
Metals separation
Electroless deposition
Hydrogenation
Hydrometallurgy
Capacitive-Faradaic fuel cells
Adsorption

ABSTRACT

The two-step catalytic process is proposed for the recovery of silver ions from aqueous solutions. First, the Ag^+-containing solution is enriched with hydrogen gas and recirculated through the Pt-loaded activated carbon (Pt/AC). The Ag^+ ions are reduced into the metal particles at ambient temperature and H_2 gauge pressure of 1 atmosphere. Next, the Ag particles precipitated on the Pt/AC are oxidized by air to form the pure Ag^+ concentrate and to regenerate the catalyst. The process was studied using pure $AgNO_3$ solutions at varied pH values (0.0, 1.5 and 3.9) in a batch mode system that was operated with Pt/AC particles loaded with 0.1–1.0% of Pt metal. The complete removal of Ag^+ ions was achieved within<2 h of hydrogenation of 1-liter $AgNO_3$ solutions with an initial concentrations of 100–1000 mgAg/L. The hydrogenation rate was not influenced by the pH value. Increasing the Pt load in the Pt/AC media above 0.25% did not result in an increase in the Ag^+ hydrogenation rate. Next, the process was applied for the separation of Ag^+ ions from H_2SO_4 leachates of Ag_2O-Zn batteries. Finally, it was shown that due to a large difference in standard reduction potentials the silver and the copper ions can be "kinetically" separated within the hydrogenation and the oxygenation steps of the process.

1. Introduction

The global annual electronic waste (e-waste) production rates in the years 2016, 2018 and 2019 were 45, 50 and 53 million metric tons, respectively [1,2]. The major producers of e-wastes are Asia, Europe, Americas, and Africa with the respective approximate contributions of 47, 24, 22, and 5 % [3]. The typical e-waste contains metals, plastics, and refractory oxides at weight ratios of 40:30:30 [4]. The metal scrap of the e-waste comprises copper (20%), iron (8%), tin (4%), nickel (2%), lead (2%), zinc (1%), silver (0.2%), gold (0.1%), palladium (0.005%) and other precious metals (e.g., tantalum, germanium, selenium and tellurium) [4,5]. Due to a high content of multiple basic and precious metals the e-waste is recognized today as an "urban mine". The estimated global value of raw materials in e-wastes generated in the year 2019 was $57 billion USD [2].

The typical e-waste recycling process starts with dismantling, followed by size reduction (using shredding, grinding, crushing and screening) into ≈ 1 cm^2 particles. Next, the particles are separated into non-metallic components, ferrous metals, and non-ferrous metals using density separators (e.g., air-classifiers, ballistic separators), magnetic separation, Eddy current separators, corona-electrostatic separation and other techniques [1,4,6]. The metallic fraction of the e-waste is processed further by hydrometallurgical, pyrometallurgical, electrometallurgical, or biometallurgical methods (and their combinations) to separate and extract pure metals/elements [5,7–9]. The most common process to date is the pyrometallurgical method which is cost effective and usually requires only a few pretreatment steps [8]. Unfortunately, the pyrometallurgical e-waste processing generates toxic furans and dioxins. The very promising biotechnological approach for the e-waste treatment is currently under a laboratory-level development [5,10].

The environmental burden of the hydrometallurgical techniques is lower than of the pyrometallurgical recovery of metals. Furthermore, process temperatures are lower which makes the hydrometallurgical approach more energy efficient. Finally, it is more selective in separation and purification of individual metals [8]. The hydrometallurgical process starts with the leaching of metals from the e-waste using nitric acid, sulfuric acid, hydrochloric acid, cyanide, halides (i.e., fluorine, chlorine, bromine, iodine, or astatine), thiourea, thiosulfate and caustic solutions [5,7]. The metals are recovered from the leachates using ion exchange [11], solvent extraction [12], precipitation and cementation [1] and other methods [7]. Although most of these methods are in industrial use, they have serious drawbacks of chemicals consumption and production

* Corresponding author.
E-mail address: ygendel@tx.technion.ac.il (Y. Gendel).

https://doi.org/10.1016/j.seppur.2021.120303
Received 30 September 2021; Received in revised form 10 December 2021; Accepted 12 December 2021
Available online 15 December 2021

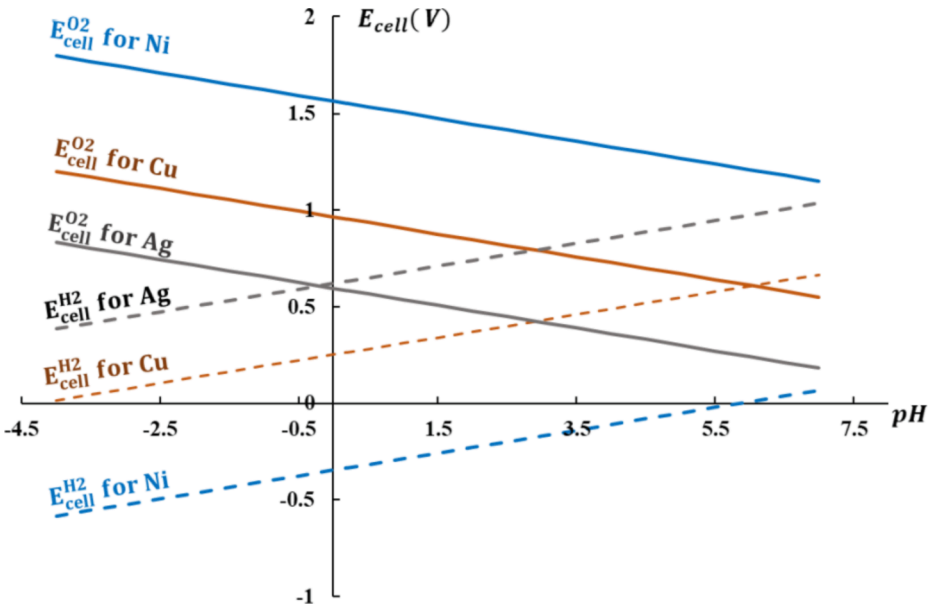

Fig. 1. Calculated Nernst potentials for hydrogenation and oxygenation of Cu^{2+}, Ag^{+} and Ni^{2+} ions ($P_{H2} = 1$ atm, $P_{O2} = 0.2$ atm, $[M^{n+}] = 1.0$ mM, 25 °C, assuming ideal gas behavior, infinite dilution and no complexation or precipitation of ionic metal species). The calculations were done using Eqs. (1–4).

of secondary wastes.

Electrodeposition can be very effective for the recovery of nickel [13], copper [14,15], silver [16–18], lead [19], tin [20] and gold [21] metals from the hydrometallurgical leachates of e-wastes. The major disadvantage of the electrodeposition technique is a low efficiency of this process for the recovery of metals from dilute solutions. For instance, high surface area electrodes (e.g., vitreous carbon) and cumbersome packed bed, fluidized bed, or spouted bed reactors must be implemented to achieve high current efficiency for copper ions recovery from solutions with [Cu] < 1 g/L [15,22–24]. This is mainly because the operation of the electrodeposition cell with dilute metal solution at high cathodic current density (typical for flat or mesh electrodes) results in energy wasting hydrogen evolution reaction.

Recently, a new catalytic technology for selective separation of copper ions from aqueous solutions was proposed by Darom and co-workers [25]. The process is performed batch-wise or continuously in a packed-bed reactor at ambient temperature and hydrogen gas gauge pressure of 1 atmosphere. The Cu-containing solution is saturated with hydrogen gas and recirculated through the catalytic media that comprises granular activated carbon loaded with nanocrystals of platinum (Pt/AC). The Pt-catalyzed reduction of copper(II) species results in precipitation of elemental Cu metal on the Pt/AC particles. At the second step of the process a separate portion of acidic aqueous solution is saturated with air and recirculated through the Cu-loaded Pt/AC catalyst. The catalytic oxygenation results in oxidation of Cu particles by oxygen into the copper(II) species to form a pure concentrate of Cu^{2+} ions. The process consumes only H_2 gas and air (as an O_2 source) and does not produce any secondary wastes. Using the Pt/AC catalyst with 0.5% platinum Darom and co-workers succeeded to separate Cu^{2+} ions from a mixture of Cu^{2+}, Ni^{2+}, Cd^{2+}, Fe^{3+}, Ca^{2+}, Mg^{2+} and Zn^{2+} ions (100 mg/L each) [25].

Besides the separation of copper ions, the new technology can be potentially applied for the recovery of other metals such as Ag^{+}, Ni^{2+}, Pb^{2+}, Bi^{3+} from aqueous solutions, including the e-waste leachates. The hydrogenation of metal-containing solution can result in the reduction of metal ions and the deposition of elemental metal (M_m) (Eq.(1)) onto the Pt/AC catalyst if the cell potential (E^{H2}_{cell}) described by the corresponding Nernst equation (Eq. (2)) is positive. The E^{H2}_{cell} value depends on the pH, temperature, hydrogen gas pressure, ionic strength, and standard reduction potential of the metal, which, in turn, depends on the nature of metal ions and on the complexation of ions by organic and inorganic ligands [26].

$$M^{n+} + 0.5nH_2 \longrightarrow M_m + nH^{+} \quad (1)$$

$$E^{H2}_{cell} = \left(E_{M_m} - E_{H2}{}^{0}\right) + \frac{R\cdot T}{n\cdot F}\ln\left(\frac{(M^{n+})(P_{H_2})^{0.5n}}{(H^{+})^{n}}\right) \quad (2)$$

$$M_m + 0.25nO_2 + nH^{+} \longrightarrow 0.5nH_2O + M^{n+} \quad (3)$$

$$E^{O2}_{cell} = \left(E_{r,O2}{}^{0} - E_{M_m}\right) + \frac{R\cdot T}{n\cdot F}\ln\left(\frac{(P_{O_2})^{0.25n}(H^{+})^{n}}{(M^{n+})}\right) \quad (4)$$

Where E_{M_m}, $E_{r,H2}{}^{0}$ and $E_{r,O2}{}^{0}$ are standard reduction potentials of metal ions (M^{n+}), protons, and oxygen, respectively; R – ideal gas constant (8.314 $\frac{J}{KA\cdot mol}$); T – temperature (K); n -charge of metal ions ($\frac{mole^{-}}{molM^{n+}}$); F – the Faraday constant (96485 $\frac{C}{mole^{-}}$); in brackets – activity and fugacity of dissolved species and gases, respectively.

The second step of the process (i.e., oxygenation of Pt/AC granules loaded with the particles of separated metal) is described by equation Eq.(3). The process is thermodynamically favorable if the corresponding Nernst potential E^{O2}_{cell} described by Eq.(4) is positive.

Fig. 1 represents the values of E^{H2}_{cell} and E^{O2}_{cell} potentials for copper ($E_{Cu_m} = 0.34$ V vs. standard hydrogen electrode, SHE), silver ($E_{Ag_m} = 0.799$ V vs. SHE), and nickel ions ($E_{Ni_m} = -0.257$ V vs. SHE) as a function of the pH in the hypothetical situation in which the metals exist in the solution as Cu^{2+}, Ag^{+} and Ni^{2+} ions (i.e., at no complexation or precipitation) and for activity and fugacity coefficients of 1.0 (i.e., infinite dilution and ideal gas conditions) (other parameters: temperature-25 °C, H_2 and O_2 absolute pressures −1.0 and 0.2 atmospheres (respectively), concentration of metals – 1.0 mM). As it is shown in Fig. 1 higher pH facilitates the reduction of metals by H_2 but hinders their oxidation by air. To make the process of Darom et al. [25] suitable for the recovery of the specific metal from water or wastewater the operational conditions (i.e., pH, temperature, pressure of gases, water composition, etc.) must be properly adjusted to make the values of both E^{H2}_{cell} and E^{O2}_{cell} potentials positive.

According to Fig. 1 the Cu^{2+} and the Ag^{+} ions can be recovered using the proposed technique at all relevant values of the pH in the treated solutions and in the produced brines. On the other hand, the Ni^{2+} ions can be reduced by hydrogen gas only if the pH is greater than 5.85. All

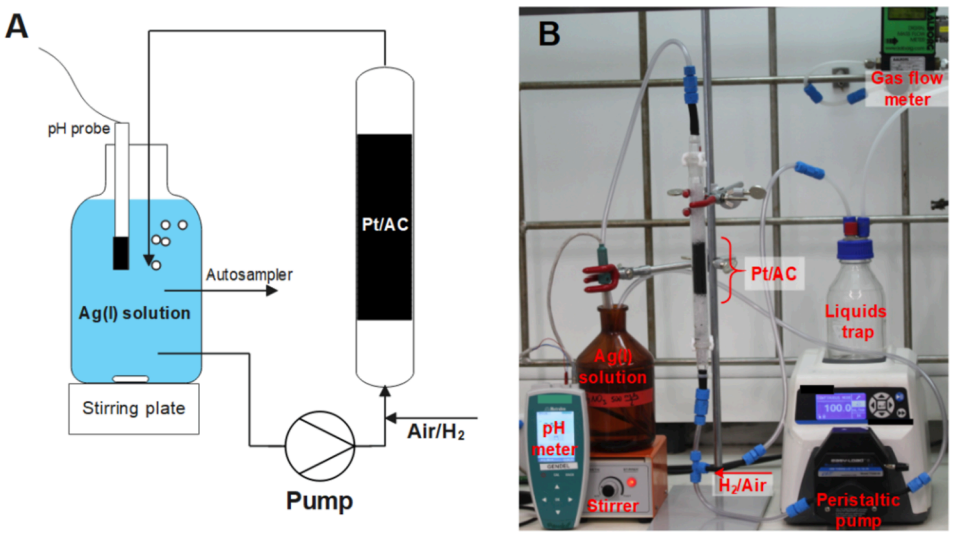

Fig. 2. The flow diagram (**A**) and the photo image (**B**) of the batch-mode experimental system applied in Ag^+ separation experiments.

three metals can be oxidized by air at ambient temperature and pressure at pH < 7.0. Thus, the Ag and the Cu metals can be separated from Ni and many other metals (i.e., Al, Fe, Cd, Zn, Pb etc.). Moreover, theoretically the hydrogenation and the oxygenation processes can be used for separation between silver and copper ions. This is due to a large difference in standard reduction potentials of silver and copper ions (i.e., +0.799 and + 0.34 V vs. SHE, respectively). Consequently, the value of E^{H2}_{cell} is by 0.46 V higher for silver than for copper. This is expected to result in much faster deposition of silver. On the other hand, the value of E^{O2}_{cell} for Cu^{2+} is by 0.46 V more positive than for Ag^+ ions. Consequently, the oxygenation is expected to result in much faster dissolution of Cu particles. This phenomenon can be applied for the separation of Ag and Cu metals as well.

The reduction of Cu^{2+}, Ni^{2+} and Ag^+ ions by the H_2 gas is thermodynamically favorable at appropriate pH, atmospheric hydrogen pressure and ambient temperature. Nevertheless, these processes require special conditions to proceed at reasonable rates. The hydrogenation of Cu^{2+} and Ni^{2+} ions in aqueous solutions is significant only at temperatures of 140–200 °C and H_2 pressure of up to 5600 kPa [27]. The Ag^+ ions cannot be hydrogenated into the atomic Ag^0 form in the solution bulk because the standard reduction potential of the Ag^+/Ag^0 pair is −1.9 V vs. SHE [28]. The previously mentioned standard reduction potential E_{Ag_m} = 0.799 V (vs. SHE) is relevant only if the Ag^0 silver is already available in the hydrogenated solution for the nucleation of new Ag^0 species [29]. To make the silver hydrogenation process thermodynamically favorable at no initial Ag^0, the polyphosphate, poly (acrylic acid) or other compounds should be used as templates that strongly bond the Ag^+ ions and make the hydrogenation thermodynamically favorable [28,29]. Darom and co-workers showed that at ambient temperature and pressure Pt/AC particles catalyze (*i*) the reduction of copper (II) species by hydrogen, and (*ii*) the oxidation of the metallic copper deposited on the Pt/AC particles by the aerial oxygen [25].

This study was dedicated to the investigation of the Pt-catalyzed hydrogenation/oxygenation process for the selective recovery of silver from dilute aqueous solutions and e-waste leachates. Another goal of the study was to prove the applicability of the process for the separation between copper and silver ions. This task is important because copper is the major metal in typical e-waste leachates. To prove the proposed concepts the catalytic process was investigated first for pure $AgNO_3$ solutions, next for the recovery of Ag from spent silver oxide-zinc (Ag_2O-Zn) batteries, and finally for the separation between Ag^+ and Cu^{2+} ions in pure $AgNO_3$ and $CuCl_2$ solutions.

2. Experimental

2.1. Preparation of the Pt-loaded granular activated carbon (Pt/AC)

The granular Pt/AC catalyst with Pt loads of 0.0, 0.1, 0.25, 0.5 and 1% (by weight) were formulated following the procedures of Amikam et al. [30,31]. Four batches of granular activated charcoal (CH104, mesh size 12–20, Spectrum) were impregnated with aqueous H_2PtCl_6 solutions at different Pt concentrations using the incipient wetness impregnation technique. Next, the carbons were dried overnight at room temperature and afterward in the oven in air atmosphere at 60 °C. The dry Pt-impregnated carbons were calcinated in N_2 atmosphere at 290 °C for 2 h and exposed to the reductive H_2 atmosphere (12 h, 300 °C) to reduce the Pt ions into the elemental Pt nanoparticles. This procedure results in Pt/AC catalysts with Pt crystals of 1–2 nm size that are uniformly distributed in activated carbon [25]. The resulting materials are further termed X%-Pt/AC, where X stands for the weight–weight percentage of the Pt content. Every portion of fresh Pt/AC catalyst was washed with a plenty of deionized water prior to the Ag removal experiments.

2.2. Experimental system

Fig. 2 shows the batch-mode system applied in this study for the investigation of the proposed process.

The Pt/AC particles (7.5 g) were localized in the glass column (internal diameter − 22.1 mm, length −25 cm) between the glass spheres (diameter of 1 mm) to prevent abrasion and loss of the catalyst during the experiments. Peristaltic pump (Masterflex, 1–600 rpm, 16″ tubing) was used to recirculate (100 mL/min) one liter of silver ions solution between the magnetically stirred amber glass bottle and the column. The PVC tubing and the column were coated with an aluminum foil (not shown in Fig. 2) to protect the solution from the sunlight. H_2 gas (99.99% purity, Maxima Ltd, Israel) and compresses air were introduced into the influent at the bottom part of the column via the T-shape connector. The flow rates of gases (180–220 mL/min) were controlled using the mass flow meters (0–1000 mL/min, Aalborg). Within every experiment the 1–2 mL samples of the solution were withdrawn periodically by the autosampler into the UV-protected plastic test tubes and analyzed later for chemical composition. The pH was recorded using the 914 EC/pH meter and 6.0228.000 glass electrode (Metrohm, Switzerland).

2.3. Investigation of Pt load influence on Pt/AC-catalyzed hydrogenation of Ag^+ ions

To study the influence of platinum content in the Pt/AC granules on the separation of silver ions the batch-mode system shown in Fig. 2 was operated with the Pt/AC (7.5 g) catalysts loaded with 0.0, 0.1, 0.25, 0.5, and 1.0% of Pt metal. Every experiment comprised at least two H_2-air cycles. First, the pure $AgNO_3$ solution (1 L, initial $[Ag^+]_0 = 500$ mg/L, $pH_0 = 0.0$ adjusted by H_2SO_4) was recirculated in the system for 3.5 h at continuous bubbling of H_2 gas. Afterwards the silver ions solution was replaced with 0.5 M H_2SO_4 solution and the system was operated for another 10 h at continuous supply of air into the column.

2.4. Investigation of pH influence on Pt/AC-catalyzed hydrogenation of Ag^+ ions

To study the effect of the pH on the catalytic separation of Ag^+ ions the system shown in Fig. 2 was operated with 1.0%-Pt/AC (7.5 g) and 1 L of $AgNO_3$ solutions with an initial concentration of 100 mgAg/L and initial pH values of 0.0, 1.5 and 3.92 (adjusted by H_2SO_4). Within every experiment the same portion of aqueous solution was applied in hydrogenation and oxygenation steps that lasted two and eight hours, respectively.

2.5. Investigation of process stability

To study the stability of the Pt-catalyzed process for Ag^+ ions separation the system shown in Fig. 2 was operated for five subsequent H_2-air cycles. The new portion of $AgNO_3$ solution ($[Ag^+]_0 = 100$ mg/L, $pH_0 = 0.0$) was used in every hydrogenation-oxygenation cycle. In cycles #1 and # 5 several granules of 1.0%-Pt/AC were withdrawn from the system after the hydrogenation and the oxygenation steps to study the composition and the morphology of the catalyst using the SEM-EDS and the XPS techniques.

2.6. Implementation of Pt-catalyzed hydrogenation-oxygenation for silver recovery from spent Ag_2O-Zn batteries

Two batches of Ag_2O-Zn batteries (SR44W, Renata 357, 1.96 g each, 11.6 X 5.4 mm size, 160 mAh nominal capacity) were discharged at constant current to the cutoff voltage of 0.2 V. The first batch of 30 cells was discharged at 2.5 mA/cell for 25.41 h, and the second batch of 10 cells was discharged at 250 μA/cell for 29.3 days. Next, the cells were dismantled, the battery powder was separated, washed with deionized water, dried at 60 °C, and milled to obtain a homogeneous material. Next, the metals were leached from the battery powder using a sulfuric acid solution which is highly effective for Ag leaching from the spent Ag_2O-Zn batteries [17,32]. To formulate the H_2SO_4 leachate the powder (5.0 g) was dissolved in H_2SO_4 solution (1 L, 0.5 M) under stirring at 70 °C for 24 h. The resulting leachate was filtered to separate undissolved metals and graphite. The supernatant was analyzed for concentration of dissolved metals and treated further for Ag^+ ions separation using the batch mode system shown in Fig. 2 (operated with 0.25%-Pt/AC, 7.5 g). The silver separated from the batteries' leachate was released within the Pt-catalyzed oxygenation step into the HNO_3 ($pH_0 = 1.0$) or H_2SO_4 solutions (0.5 M). In three sets of experiments the ratios between the volume of the leachate to the volume of the concentrate ($\frac{V_{leachate}}{V_{concentrate}}$) were 1, 5 and 10 (in last two experiments the leachate was diluted with 0.5 M H_2SO_4). Finally, the metallic silver was electrodeposited from the concentrates obtained in Pt-catalyzed process using the three-electrode cell with a platinum plate (1·2.5 cm·cm) anode and cathode, and Ag/AgCl (3.0 M KCl) reference electrode. The constant current of 100 mA (i.e., current density of 20 mA/cm^2) was supplied by the PGSTAT302N Autolab potentiostat/galvanostat.

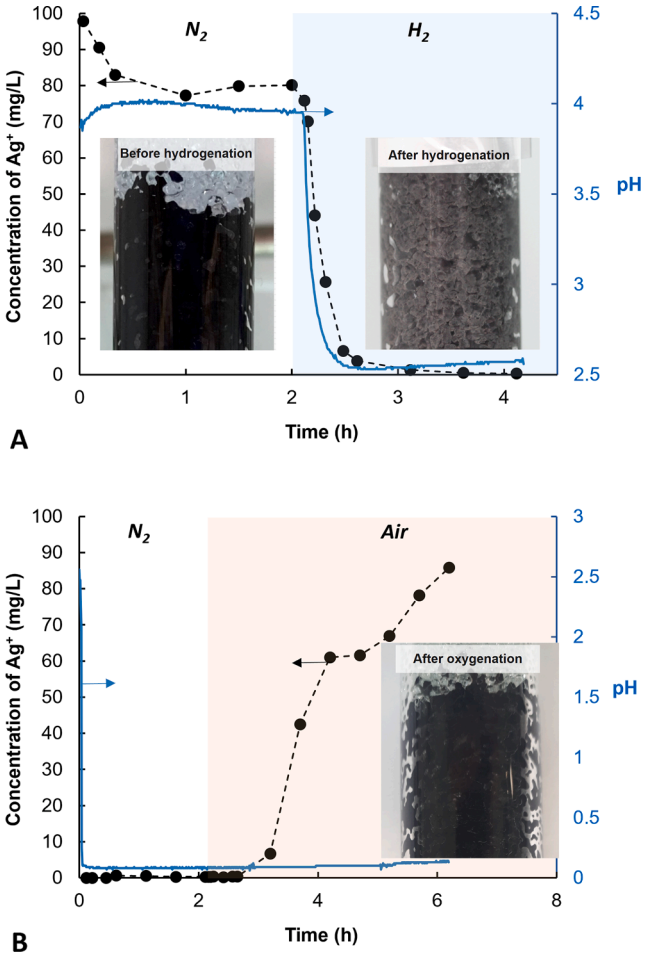

Fig. 3. Concentration of Ag^+ ions and pH versus time in $AgNO_3$ solution (1 L, $[Ag]_0 = 100$ mg/L, $pH_0 = 3.87$) purged with N_2 and H_2 gases in a batch mode system with 7.5 g of 1.0%-Pt/AC catalyst (**A**). Next, the $AgNO_3$ solution was replaced with H_2SO_4 (1 L, 0.5 M) and the system purged with N_2 gas and air (**B**). Temperature 20–25 °C; N_2, H_2, and air gauge pressure – 1 atm; gas flow rate −180–220 mL/min. Inserts - photo images of the catalytic media before Ag^+ ions separation, after hydrogenation and after oxygenation.

2.7. Analytical methods

Concentrations of Ag^+, Mn^{2+}, Fe^{3+} and Zn^{2+} ions were determined using the ICP-OES technique (PlasmaQuant PQ 9000 Elite, Analytik Jena AG). The concentration of Cu^{2+} was determined by the method of Wen et al. [33]. The Ag-containing deposits on the Pt/AC catalysts and on the geotextile cloth were examined by the high-resolution field emission Gun SEM ZEISS Ultra Plus equipped with EDS Oxford Instruments (England). The EDS measurements were carried out using the acceleration voltage of 5 kV, the probe current of about 0.5nA at the working distance of 8.5 mm. The take-off angle of X-ray radiation was 35°. The acquisition time was 50 s per single measurement. The standard deviation of the measured intensity for a single measurement did not exceed 5 %. Quantitative analysis was performed using the conventional correction procedure included in the INCA software. Results of chemical composition (atomic %) were normalized to 100 %.

The X-ray Photoelectron Spectroscopy (XPS) measurements were performed in UHV ($2.5x10^{-10}$ Torr base pressure) using 5600 Multi-Technique System (PHI, USA). The sample was irradiated with an Al Kα monochromated source (1486.6 eV) and the outcome electrons were analyzed by a Spherical Capacitor Analyzer using the slit aperture of 0.8 mm. The samples were analyzed at the surface only. Charge neutralization was used to match C1s peak to 284.8 eV. Sputtering was done at a

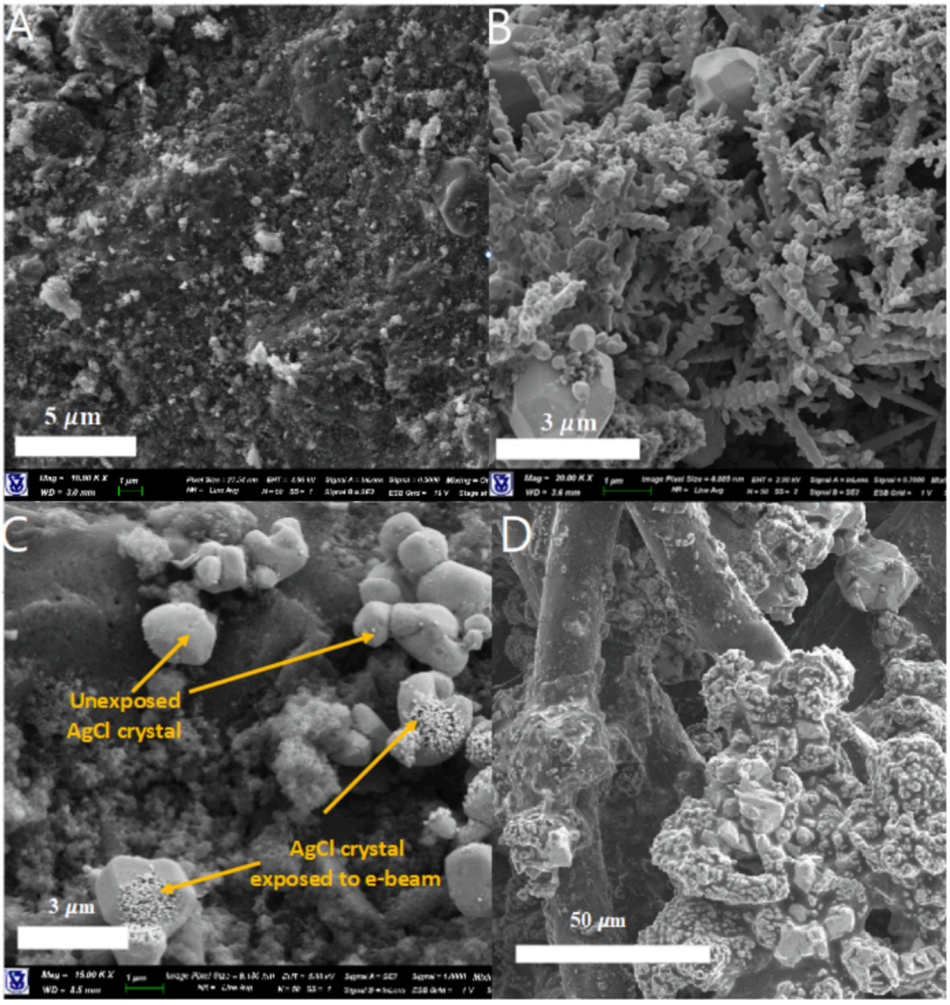

Fig. 4. The SEM images of (**A**) Pt/AC particle surface before hydrogenation; (**B**) after 2.12 h of catalytic hydrogenation of pure $AgNO_3$ solution (1 L, $[Ag]_0 = 100$ mg/L) with 7.5 g of 1.0%-Pt/AC, and (**C**) after oxygenation in H_2SO_4 solution (1 L, 0.5 M). (**D**) – The SEM image of the geotextile filter after the hydrogenation – oxygenation cycle.

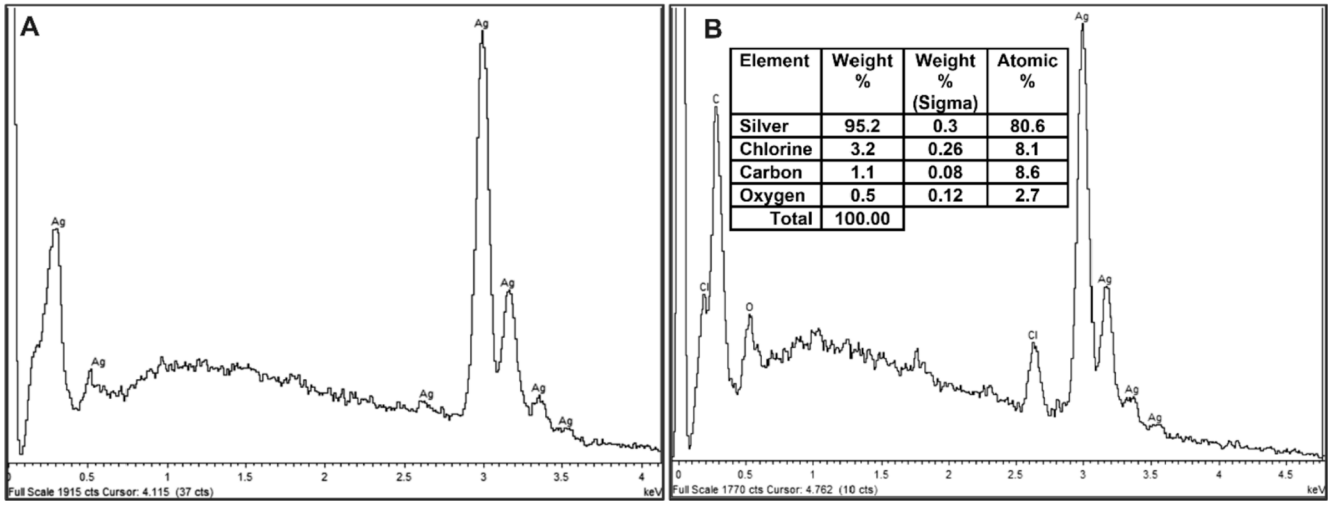

Fig. 5. The results of SEM/EDS analysis of Ag-containing deposits formed on the 1.0%-Pt/AC catalyst during the hydrogenation of $AgNO_3$ solution (1 L, $[Ag]_0 = 100$ mg/L) (**A**), and after the oxygenation of the Ag-loaded Pt/AC media in H_2SO_4 (1 L, 0.5 M) solution (**B**).

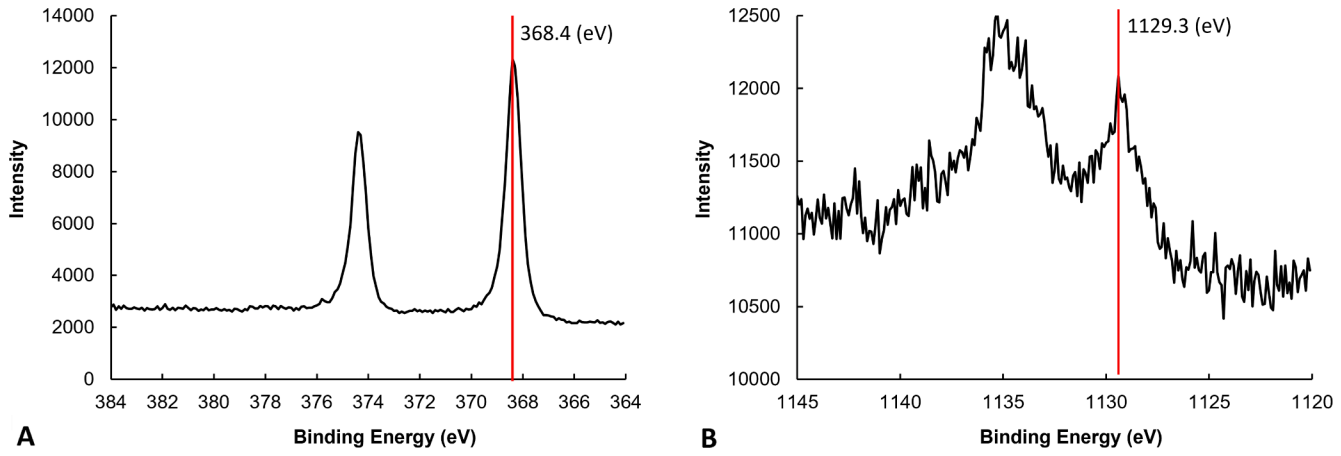

Fig. 6. The XPS spectrum of Ag3d level (**A**) and the AgMVV Auger spectrum (**B**) of silver particles formed on 1.0%-Pt/AC catalyst during the hydrogenation of $AgNO_3$ solution (1 L, $[Ag]_0 = 100$ mg/L).

rate of 47.6 A/min (calibrated for SiO_2).

3. Results

3.1. Proof-of-concept

Fig. 3 shows the results of the proof-of-concept experiment of Ag^+ ions recovery by the proposed process.

In this experiment the system shown in Fig. 2 was operated with 7.5 g of 1.0%-Pt/AC catalyst to recover the silver ions from the $AgNO_3$ solution (1 L, $[Ag]_0 = 100$ mg/L, $pH_0 = 3.87$) into the H_2SO_4 solution (1 L, 0.5 M). Recirculation of $AgNO_3$ solution for two hours through the Pt/AC column under the N_2 gas purging resulted in the decrease of Ag^+ ions concentration from 100 mg/L to 80 mg/L (Fig. 3A).

The adsorption of Ag^+ ions by activated carbons was previously reported by Jia and Demopoulos [34]. The silver ions separated from aqueous nitrate and sulfate solutions were found on the activated carbon in the reduced Ag^0 form due to the reduction of Ag^+ ions by the hydroquinone-like surface oxygen functional groups [34]. Another mechanism of Ag^+ separation was postulated to be the ion-exchange on the carboxylic groups [34]. The N_2-step of the experiment shown in Fig. 3 resulted in adsorption density of Ag on the Pt/AC catalyst of ≈ 0.025 mmol/g. This value is approximately 20 times lower than the Ag adsorption density reported by Jia and Demopoulos (i.e., ≈ 0.45 mmol/g) for $AgNO_3$ solution with $pH_0 = 4.5$ [34]. The significantly lower adsorption density obtained in the present study is probably due to the thermal treatment of carbons applied for Pt loading. Once the hydrogen gas was introduced into the system (Fig. 3A) the concentration of Ag^+ ions decreased to 0.0 mg/L within 2.12 h of the hydrogenation, that corresponds to the adsorption density of ≈ 0.12 mmol/g. During the hydrogenation the catalytic Pt/AC media was covered with the gray layer of metallic silver visible to the naked eye (Fig. 3A). Next, the $AgNO_3$ solution was replaced with H_2SO_4 (0.5 M, 1 L) and the N_2 gas was supplied into the system for 2 h. As it is shown in Fig. 3B no Ag^+ ions

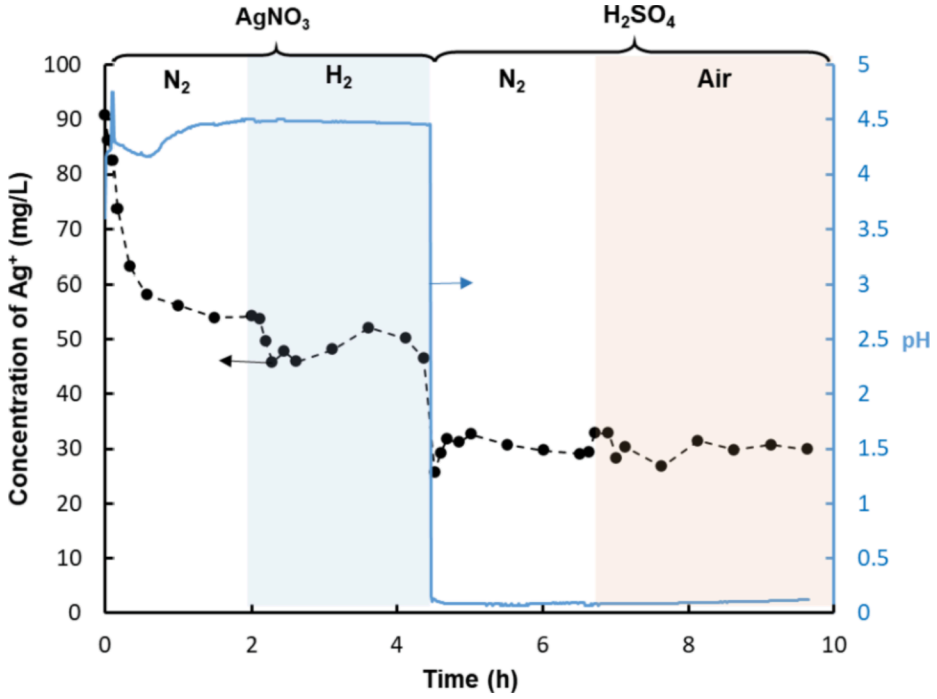

Fig. 7. Results of Ag^+ ions recovery from pure $AgNO_3$ solution (1 L, $[Ag]_0 = 100$ mg/L, $pH_0 = 3.87$) into H_2SO_4 solution (1 L, 0.5 M) using a batch mode system operated with 7.5 g of pristine granular activated charcoal. Temperature 20–25 °C; N_2, H_2, and air gauge pressure – 1 atm, gas flow rate 180–220 mL/min.

were released into the H_2SO_4 solution with N_2 gas in the system. The introduction of air into the system resulted in oxidation of metallic Ag on the Pt/AC catalyst and 90% of Ag^+ ions initially present in the system were obtained in the H_2SO_4 solution after 4 h of the oxygenation (Fig. 3B). After the oxygenation the catalytic media lost the visible metallic silver layer. Fig. 4A and 4B show the SEM images of Pt/AC surface before and after the hydrogenation, respectively. The typical EDS spectra of crystals formed on Pt/AC catalyst after the hydrogenation and the oxygenation of $AgNO_3$ solution are presented in Fig. 5.

All distinct peaks in the EDS spectrum shown in Fig. 5A belong to silver. Concentrations of all other elements in the Ag-layer formed within the hydrogenation step were below the detection limit. In addition, analyzed crystals were not sensitive to prolonged irradiation during the EDS analysis.

The XPS analysis was employed to determine the chemical state of silver in the particles formed on the surface of Pt/AC granules within the catalytic hydrogenation of $AgNO_3$ solution. Fig. 6A shows the high resolution XPS spectrum for binding energies (BE) associated with the Ag3d region of the sample. The peaks situated at 374.3 eV and 368.4 eV appear due to the spin orbital splitting that correspond to $Ag3d_{3/2}$ and $Ag3d_{5/2}$ levels, respectively. The most accurate value of the $Ag3d_{5/2}$ peak for solid silver is 368.327 eV for the Al Kα monochromated source (1486.6 eV) [35,36]. The value of 368.4 eV obtained in this study for the $Ag3d_{5/2}$ peak is slightly higher than 368.327 eV that proves that catalytic hydrogenation of $AgNO_3$ solution leads to formation of Ag^0 silver [35]. This conclusion also follows from the value of Auger parameter (AP) that can be calculated from the values of $Ag3d_{5/2}$ (Fig. 6A) and AgMVV (Fig. 6B) peaks as AP = BE + KE = 368.4 + (1486.6–1129.3) = 725.7 eV (KE is the Auger kinetic energy). This value is very close to the AP of 726.182 eV that was previously determined for solid silver [35,36].

The SEM analysis showed that the Ag crystals formed within the H_2 step completely disappeared from the Pt/AC surface after 6 h of aeration. However, the AgCl crystals were obtained on the surface of the Pt/AC media after the oxygenation step (Fig. 4C and Fig. 5B). Silver chloride crystals are sensitive to the electron beam irradiation that caused the destruction of AgCl particles during the SEM-EDS analysis (Fig. 4C). The origin of chloride ions in the system is the KCl (3.0 M) electrolyte solution of the glass pH electrode that was immersed in the $AgNO_3$ solution for the whole duration of the experiment. Another possible source of the Cl^- ions is the activated carbon.

Fig. 7 shows the results of Ag^+ ions separation experiment conducted with pristine activated charcoal at operational conditions like those applied in the experiment shown in Fig. 3. As it is shown in Fig. 7 almost 55% of the Ag^+ ions were removed by the carbon that corresponds to the adsorption density of 0.068 mmol/g which is still much lower than the values reported by Jia and Demopoulos [34]. This is apparently because two different types of carbons were applied in these studies.

Introduction of H_2 gas did not result in any significant change in (reductive) adsorption of Ag^+ ions, nor in the pH value of the $AgNO_3$ solution. The replacement of the $AgNO_3$ solution with the N_2-purged H_2SO_4 solution (1 L, 0.5 M) resulted in the release of some Ag^+ ions from the carbon (Fig. 7). This is due to reoxidation of Ag^0 and/or because the carbon surface became more positive in the low-pH solution [34]. Aeration of the H_2SO_4 solution did not result in any additional release of Ag^+ ions (Fig. 7). The differences between the results obtained in experiments conducted with the Pt-loaded carbon (Fig. 3) and the pristine activated carbon particles (Fig. 7) indicate on different mechanisms that govern the Ag^+ ions separation in these two experiments. It is important to emphasize that the Pt-loaded activated carbon can be easily regenerated by the oxygenation with air and reused in the next cycle of the Ag^+ ions separation. This cannot be done with the pristine Pt-free activated carbon. Moreover, the presence of zinc ions (which is common in leachates of Ag_2O-Zn batteries) hinders the Ag^+ separation by unmodified carbons [34].

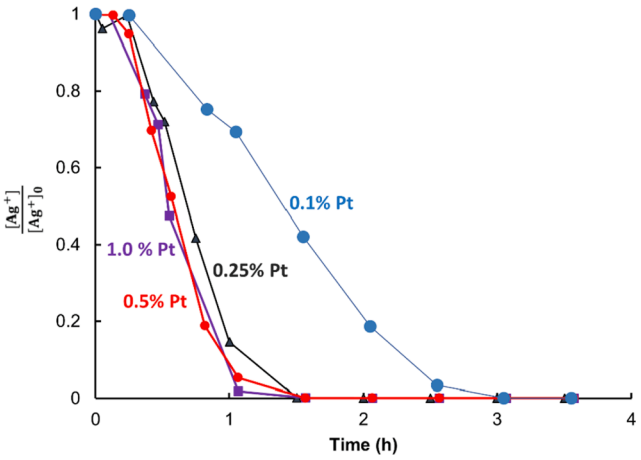

Fig. 8. Results of the Ag^+ ions hydrogenation in $AgNO_3$ solution (1 L, $[Ag]_0$ = 500 mg/L, pH_0 = 0.0) using a batch mode system operated with 7.5 g of granular activated charcoal loaded with 0.1, 0.25, 0.5 and 1.0 % of platinum. Temperature 20–25 °C; H_2 and air gauge pressure – 1 atm; H_2 and air flow rates 180–220 mL/min.

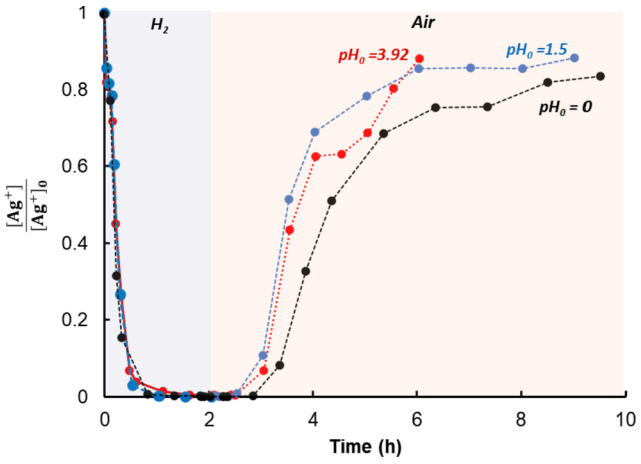

Fig. 9. Variation of Ag^+ ions concentration with time within hydrogenation-oxygenation experiments conducted with 7.5 g of 1.0 %Pt-AC and $AgNO_3$ solutions (1 L, $[Ag]_0$ = 100 mg/L) at varied initial pH values of 0.0, 1.5 and 3.92. Temperature 20–25 °C; H_2 and air gauge pressure – 1 atm; H_2 and air flow rates 180–220 mL/min.

3.2. The influence of the Pt load in the Pt/AC catalytic media on the removal of silver ions

Fig. 8 shows the results of the $AgNO_3$ hydrogenation experiments conducted using the batch mode system (Fig. 2) with 1 L of $AgNO_3$ solution ($[Ag^+]_0$ = 500 mg/L, pH_0 = 0.0) and Pt/AC catalysts with Pt loads of 0.1, 0.25, 0.5 and 1.0 %.

In all four tests the complete separation of silver ions was achieved that corresponds to the adsorption density of 0.618 mmolAg/g, which is significantly higher than the adsorption density of ≈ 0.45 mmol/g reported by Jia and Demopoulos [34] for the un-modified activated carbon.

The hydrogenation rate of Ag^+ ions by the Pt/AC catalyst with the Pt load of 0.1% was significantly lower than for the catalysts with Pt load higher than 0.25%. On the other hand, the hydrogenation performance was almost the same for activated charcoals with Pt loads of 0.25, 0.5 and 1.0%, i.e., all Ag^+ ions were removed within ≈ 1.5 h. Optimization studies are required to increase the utilization efficiency of the Pt catalyst and to decrease the capital cost of the proposed process.

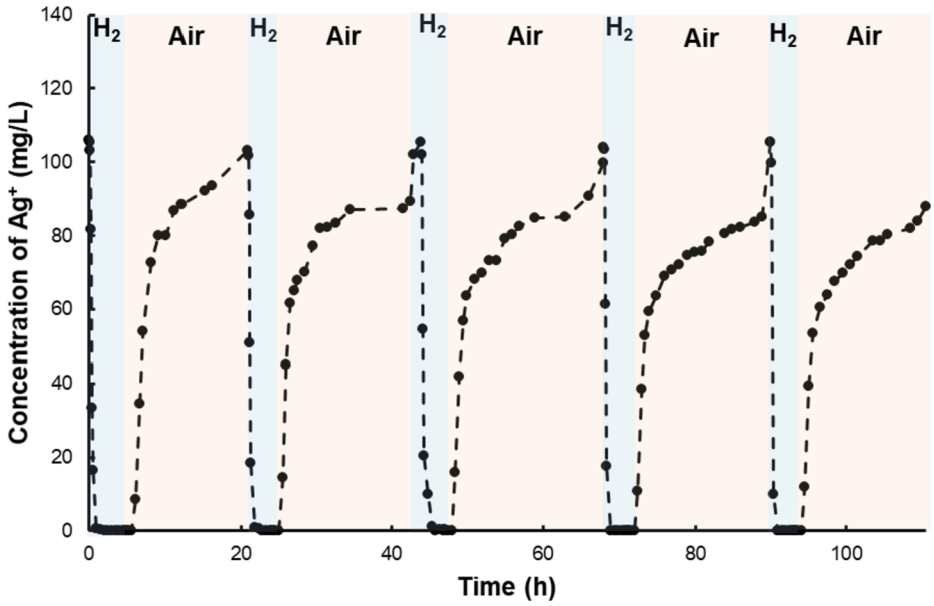

Fig. 10. Results of five hydrogenation-oxygenation cycles of Ag^+ ions recovery from the $AgNO_3$ (1 L, $[Ag^+]_0 = 100$ mg/L, $pH_0 = 0.0$) solution into the H_2SO_4 (1 L, 0.5 M) solution using the batch-mode system operated with 7.5 g of 1.0%-Pt/AC catalyst. Temperature 20–25 °C; H_2 and air gauge pressure – 1 atm; H_2 and air flow rates 180–220 mL/min.

3.3. The influence of pH on Ag^+ ions removal by the Pt/AC-catalyzed hydrogenation.

Fig. 9 concentrates the results of batch mode hydrogenation-oxygenation experiments conducted with 7.5 g of 1.0 %Pt-AC catalyst and $AgNO_3$ solutions (1 L, $[Ag^+]_0 = 100$ mg/L) at initial pH values of 0.0, 1.5 and 3.92. As it is shown in Fig. 9 in all experiments more than 90% of silver ions were removed within the first hour of the hydrogenation. The reduction rates were similar at three tested pH values. The effect of the pH on the oxygenation rate cannot be obtained from the collected data. This is because there is a relatively long transition period between the hydrogenating to the oxygenating conditions in the applied experimental system that makes the comparison of the data inaccurate. In all three experiments the oxygenation for 6.5 h resulted in the release of $\geq$ 80% of the silver into the concentrate solution. The Ag^+ ions removed within the hydrogenation step could not be completely recovered by the oxygenation. This is due to the detachment of the metallic Ag particles from the Pt/AC media during the hydrogenation step of the process. Some detached Ag particles were observed at the bottom of the $AgNO_3$ solution vessel after the termination of the experiment.

3.4. Stability of the process for silver ions removal

Fig. 10 shows the variation of Ag^+ ions concentration as a function of time in five consecutive hydrogenation-oxygenation experiments conducted using the batch mode system (Fig. 2) that was operated with the same portion of Pt/AC catalyst (7.5 g, 1.0% platinum load). Fresh $AgNO_3$ (1 L, $[Ag^+]_0 = 100$ mg/L, $pH_0 = 0.0$) and H_2SO_4 (1 L, 0.5 M) solutions were applied in every hydrogenation-oxygenation cycle. In all five cycles the silver ions were completely removed from the $AgNO_3$ solution during the hydrogenation. However, only 82.2% to 86.8% of the silver ions were converted from the $AgNO_3$ solution into the H_2SO_4 solution. The incomplete recovery of the Ag^+ ions is attributed to the detachment of metallic Ag particles from the Pt/AC media during the hydrogenation step of the process.

Table 1
Concentrations of metals in the leachates of spent Ag_2O-Zn cells discharged at constant currents of 2.5 mA/cell and 250 μA/cell to the cut-of voltage of 0.2 V (solid to liquid ratio in powder leaching = 5 g/L).

Discharge conditions	Leached metal (weight % in dry battery powder)		
	Ag	Zn	Mn
Cells discharged at 2.5 mA/cell for 25.41 h.	28.98	25.6	11.76
Cells discharged at 250 μA/cell for 29.3 days.	26.5	23.67	19.85

3.5. Implementation of the process for silver recovery from spent Ag_2O-Zn batteries

Table 1 lists the composition of leachates obtained after 24-hour long dissolution of metals from the powder of spent Ag_2O-Zn batteries using the H_2SO_4 (0.5 M, 70 °C) lixiviant.

The discharge of the Ag_2O-Zn batteries at 2.5 mA/cell and 250 μA/cell currents resulted in the apparent discharge capacities of 39.7% and 109.8 % (respectively) out of the nominal capacity of 160 mAh. Equations (5)-(8) describe the reactions that occur on an anode and on a cathode of Ag_2O-Zn cells during a discharge in alkaline NaOH electrolyte solution [17].

Anode:

$$ZnO + H_2O + 2e^- \rightarrow Zn + 2OH^- \quad (E_r^0 = -1.249 \text{ V vs. SHE}) \tag{5}$$

Cathode:

$$Ag_2O + 2H^+ + 2e^- \rightarrow 2Ag + H_2O \quad (E_r^0 = 0.342 \text{ V vs. SHE}) \tag{6}$$

$$2MnO_2 + H_2O + 2e^- \rightarrow Mn_2O_3 + 2OH^- \quad (E_r^0 = 0.150 \text{ V } vs. \text{ SHE}) \tag{7}$$

The MnO_2 is added into a cathode of Ag_2O-Zn cells to lower a content of the expensive silver [17]. Consequently, the powder of a spent battery is expected to contain Ag, Ag_2O, Zn, ZnO, MnO_2 and Mn_2O_3 species. The metals and oxides are leached from the spent cells by the H_2SO_4 solution into Ag^+, Zn^{2+} and Mn^{2+} via Eqs. (8)–(11) [17]. The cells discharged at

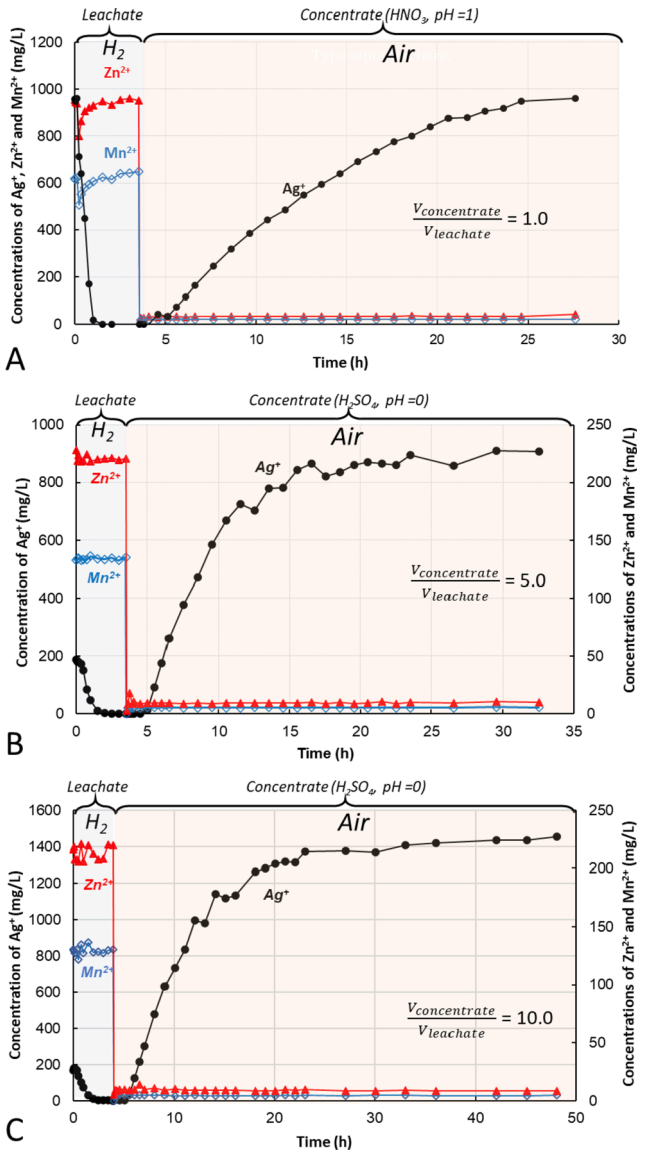

Fig. 11. Results of Pt-catalyzed separation of Ag^+ ions from the leachate of Ag_2O-Zn batteries at $\frac{V_{leachate}}{V_{concentrate}}$ ratios of 1.0 **(A)**, 5.0 **(B)**, and 10.0 **(C)**. Conditions: 7.5 g of 0.25 %Pt-AC; temperature 20–25 °C; H_2 and air gauge pressure – 1 atm; H_2 and air flow rates- 180–220 mL/min.

250 μA/cell comprise silver mostly in the metallic Ag^0 form that is insoluble in H_2SO_4 solutions. The cells discharged at 2.5 mA/cell contain both the Ag^0 metal particles and the Ag_2O oxide which is soluble in H_2SO_4 (Eq. (8)). The concentrations of the Ag^+ ions in two leachates were almost identical (Table 1). This is due to the oxidation of the Ag metal in the discharged cells by MnO_2 oxide via Eq. (10) [17]. The Mn_2O_3 that is formed during a discharge of Ag_2O-Zn cells can also take a part in leaching of Ag metal via Eq. (12) or/and it can be dissolved first into MnO_2 and Mn^{2+} species via the reaction Eq. (13) [37,38].

$$Ag_2O + 2H^+ \rightarrow 2Ag^+ + H_2O \quad (8)$$

$$ZnO + 2H^+ \rightarrow Zn^{2+} + H_2O \quad (9)$$

$$MnO_2 + 2Ag + 4H^+ \rightarrow Mn^{2+} + 2H_2O + 2Ag^+ \quad (E^0 = 0.424\ V) \quad (10)$$

$$Zn + 2H^+ \rightarrow Zn^{2+} + H_2 \quad (E^0 = 0.762\ V) \quad (11)$$

$$Mn_2O_3 + Ag + 6H^+ \rightarrow 2Mn^{2+} + Ag^+ + 3H_2O \quad (E^0 = 0.686\ V) \quad (12)$$

$$Mn_2O_3 + 2H^+ \rightarrow Mn^{2+} + MnO_2 + H_2O \quad (13)$$

The lower content of Mn^{2+} in the leachate of cells partially discharged at 2.5 mA/cell is apparently because the solubility of MnO_2 is significantly lower than the solubility of Mn_2O_3 [37,38].

Fig. 11 shows the results of batch mode experiments aimed to prove the capability of the proposed Pt-catalyzed process to selectively separate Ag^+ ions from the leachates of Ag_2O-Zn batteries. The Ag recovery tests shown in Fig. 11 were performed using the batch mode system (Fig. 2) that was operated with 7.5 g of 0.25%-Pt/AC particles, 1 L of mixed leachate solutions, and 1 L of HNO_3 (pH_0 = 1.0) concentrate solution. The mixed leachate was obtained by mixing the H_2SO_4 leachate of batteries discharged at 2.5 mA/cell (1.5 L) and batteries discharged at 250 μA/cell current (2.0 L). In experiments shown in Fig. 11B and Fig. 11C the mixed leachate was diluted 1/5 with 0.5 M H_2SO_4 solution. As it is shown in Fig. 11 the complete recovery of Ag^+ ions from the H_2SO_4 leachate was achieved in all three experiments. The adsorption density as high as 1.18 mmolAg/g was obtained. The final concentrations of Mn^{2+} and Zn^{2+} ions in the hydrogenated leachates were practically identical to their initial concentrations. In experiments conducted with $\frac{V_{leachate}}{V_{concentrate}}$ ratios of 1 and 5 (Fig. 11A and 11B) approximately 100% and 95.4% (respectively) of the silver was transferred into the concentrate solutions by the oxygenation. However, in the experiment conducted with $\frac{V_{leachate}}{V_{concentrate}}$ ratio of 10 (Fig. 11C) only 71.8% of the silver was found in the concentrate. The incomplete conversion is due to the detachment of Ag metal particles from the Pt/AC media that (for an unclear reason) was very intensive in this experiment. The Ag metal particles (152.7 mg) were separated from the treated leachate solution by filtration.

The overall amount of silver metal recovered from the batteries' leachate (i.e., found in the dissolved form in the concentrate and separated as the Ag^0 metal particles from the hydrogenated leachate) was ≈ 88%. The rest 12% of the silver metal was accumulated on the surface of tubing, glass spheres, and other parts of the system. The phenomenon of Ag particles detachment should be properly investigated for further development of the proposed catalytic process. In general, the detachment is not problematic for the silver recovery, but the process must include a properly designed filtration unit to collect the detached silver particles.

The purity of silver ions in the concentrates (calculated as $\frac{[Ag^+]}{[overall\ metals]}$ ratio) obtained in the Pt-catalyzed experiments with $\frac{V_{leachate}}{V_{concentrate}}$ ratios of 1, 5 and 10 was 93.6%, 98.34% and 99%, respectively. The minor amounts of Mn^{2+} and Zn^{2+} were present in the Ag concentrate solutions (Fig. 11) because no washing of the Pt/AC media was applied after the hydrogenation step of the process.

The electrodeposition experiments were performed to demonstrate the extraction of metallic silver from the concentrates that had been formed within the Pt-catalyzed recovery of Ag^+ ions from the leachates of spent Ag_2O-Zn batteries. The concentrates were electrolyzed at the constant current density of 20 mA/cm^2 using the three-electrode cell with the Pt-made cathode and anode. Fig. 12 shows the results of the electrodeposition experiment conducted with the concentrate formed within the Pt-catalyzed Ag recovery at $\frac{V_{leachate}}{V_{concentrate}}$ ratio of 10. As it is shown in Fig. 12A 96% of silver ions were reduced on the cathode into the metallic silver within 108 min of the electrodeposition (Fig. 12B). No decrease in concentrations of Mn^{2+} and Zn^{2+} ions was observed. The depletion of the Ag^+ ions in the electrolyte solution was accompanied by the sharp decrease in the cathodic potential (Fig. 12A).

3.6. Separation of Cu^{2+} and Ag^+ ions using the Pt-catalyzed hydrogenation-oxygenation

Fig. 13 concentrates the results of Pt-catalyzed hydrogenation-oxygenation experiment that was conducted in the batch mode system

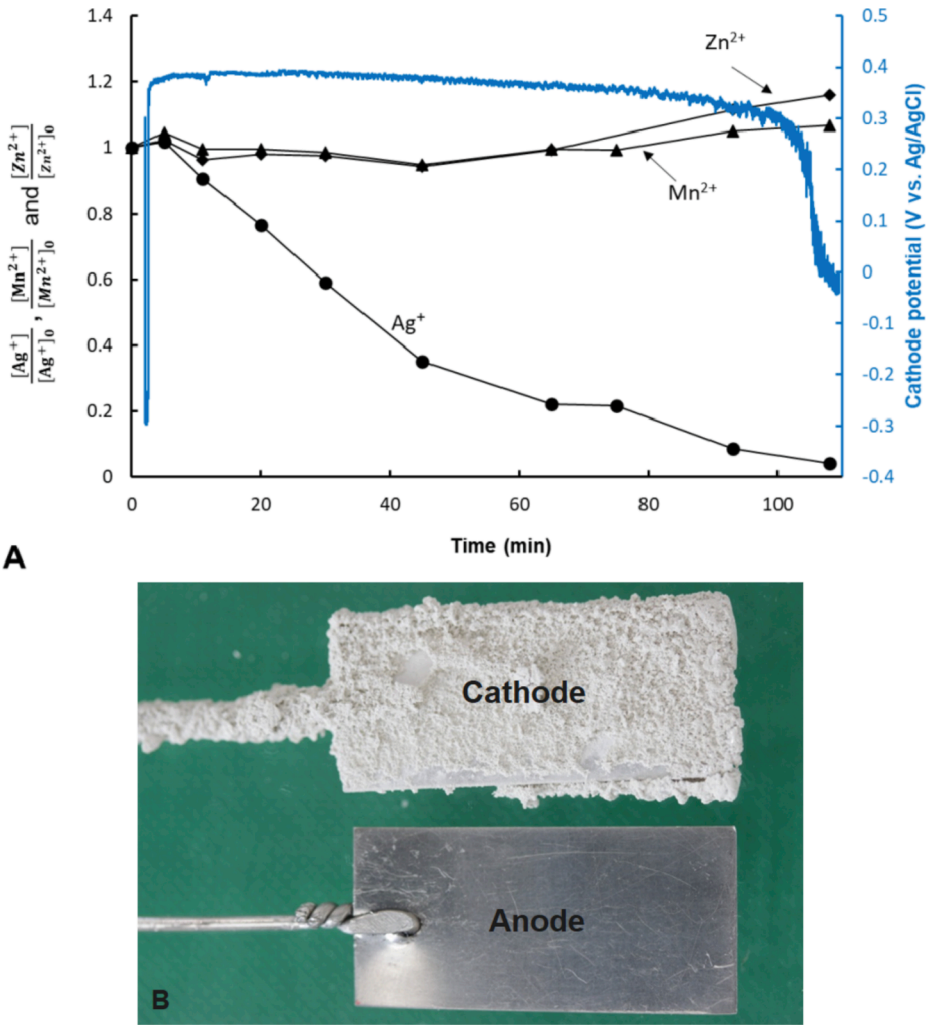

Fig. 12. (**A**) Concentration of Ag^+, Mn^{2+} and Zn^{2+} ions versus time during the electrodeposition in the concentrate of the Pt-catalyzed extraction of Ag from the leachate of spent Ag_2O-Zn batteries ($\frac{V_{leachate}}{V_{concentrate}} = 10$, Fig. 11C). (**B**) The photo images of the anode and the cathode after the electrodeposition of silver.

shown in Fig. 2 with 7.5 g of 0.25 %Pt-AC catalyst and acidic solution (1.0 L, $pH_0 = 0.0$ adjusted by H_2SO_4) that contained $AgNO_3$ (250 mgAg/L) and $CuSO_4$ (250 mgCu/L).

As it is shown in Fig. 13A, the concentration of silver ions started to decrease linearly with time immediately with the beginning of the hydrogenation step. After 50 min of the hydrogenation 6% and 99.99% of copper and silver ions (respectively) were removed from the Ag^+-Cu^{2+} mixture (line A in Fig. 13A). This corresponds to the purity of the deposited silver of ≈ 94%. Fig. 13B shows the photo images of the catalytic media. The Pt/AC catalyst became coated with a gray layer of silver metal after the hydrogenation step (Fig. 13A). The concentration of the Cu^{2+} ions decreased by 6% within the first two minutes of the experiment and the Cu^{2+} concentration remained constant until all silver ions were removed from the solution. Immediately after the complete removal of Ag^+ ions from the solution the concentration of Cu^{2+} ions started to decrease linearly with time and all Cu^{2+} ions were removed from the solution after 1 h and 50 min. The Pt/AC catalyst became coated with the reddish-brown layer of the metallic copper (Fig. 13B). The results shown in Fig. 13 prove that Ag^+ and Cu^{2+} ions can be separated by the Pt-catalyzed hydrogenation because silver ions are reduced much faster than copper ions.

The oxygenation of the solution resulted in complete release of copper that was followed by the release of silver ions (Fig. 13). Oxygenation for 5 h and 49 min (marked by line B in Fig. 13A) resulted in the release of 103% of copper and only 0.35 % of silver from the catalytic media. In parallel, the catalyst lost the reddish-brown color of copper (Fig. 13B). The purity of copper in the treated solution at this point of the experiment was 99.54%. The oxygenation of silver started only after the release of copper from the catalytic media had been completed. All the silver was oxidized within ≈ 7 h of the oxygenation (Fig. 13A). Consequently, the Ag^+ and Cu^{2+} ions can be separated by the proposed catalytic process during its hydrogenation and/or oxygenation steps.

4. Conclusions

In this study we have shown for the first time that silver ions (Ag^+) can be catalytically reduced in aqueous solutions into the elemental Ag^0 metallic form by the hydrogen gas at ambient temperature and H_2 gauge pressure of 1 atmosphere. Complete separation of Ag^+ ions from 1-liter $AgNO_3$ solutions ($[Ag^+]$ of 100 to1000 mg/L) was achieved in a batch mode system that was operated with 7.5 g of Pt-loaded activated carbon catalysts. Experiments conducted with granular activated carbon loaded with 0.1, 0.25, 0.5 and 1.0 % Pt metal have shown that increasing the Pt load beyond 0.25% did not result in faster kinetics of Ag^+ ions reduction. Similar hydrogenation rates of Ag^+ ions were obtained in $AgNO_3$ solutions ($[Ag^+]_0 = 100$ mg/L) with the initial pH values of 0.0, 1.5 and 3.92. Some Ag particles were detached from the catalytic media during the hydrogenation step of the process. The oxygenation of the Ag-loaded Pt/AC catalytic media in H_2SO_4 solutions resulted in oxidation of the

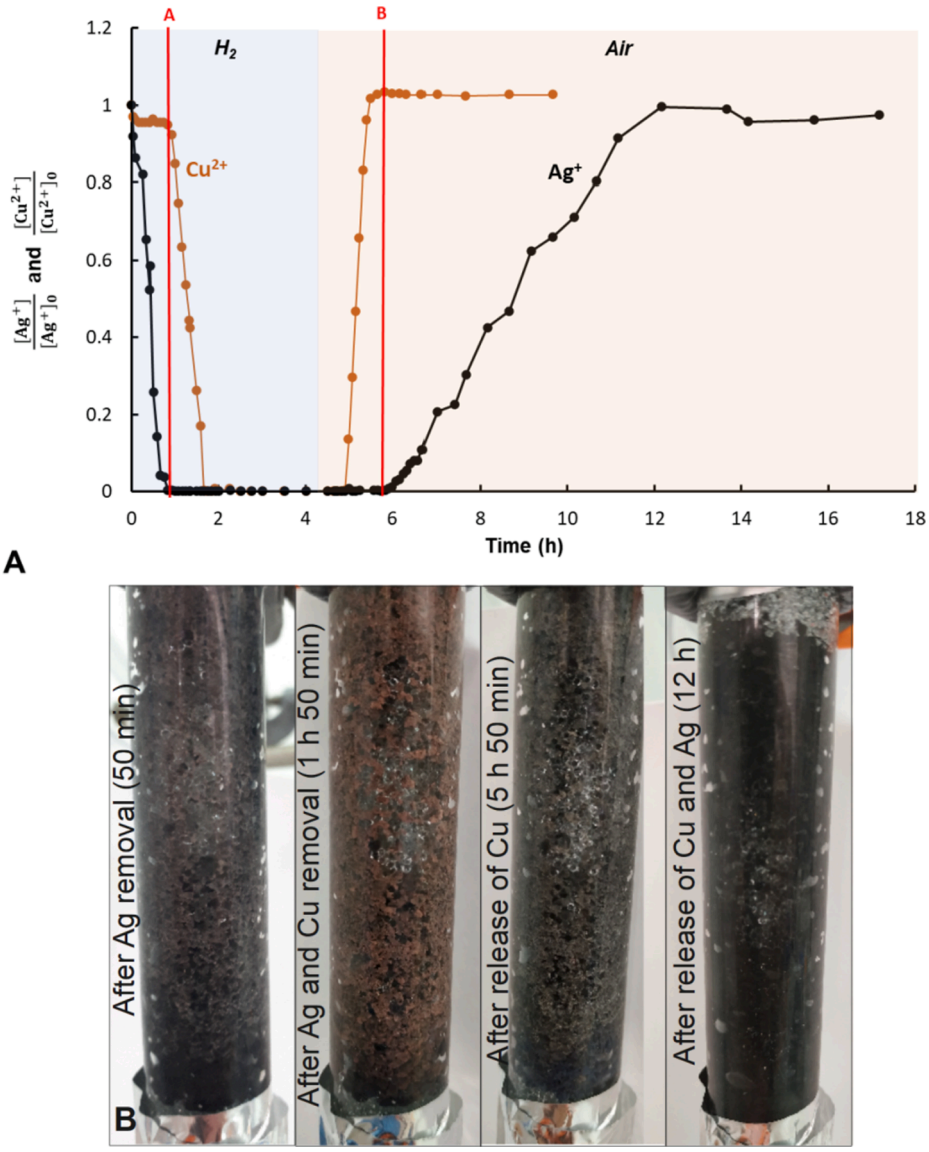

Fig. 13. (**A**) Concentrations of Ag^{+} and Cu^{2+} ions versus time during the hydrogenation-oxygenation cycle of solution (1.0 L) that comprised $AgNO_3$ (250 mgAg/L) and $CuSO_4$ (250 mgCu/L). Conditions: pH_0 = 0.0; 7.5 g 0.25 %Pt-AC catalyst; temperature 20–25 °C; H_2 and air gauge pressure – 1 atm; H_2 and air flow rates 180–220 mL/min. (**B**) The photo images of the catalytic bed during four different stages of the process.

silver into the Ag^{+} ions. The catalytic hydrogenation-oxygenation process was successfully implemented for the separation of silver from the H_2SO_4 leachates of spent Ag_2O-Zn batteries. It was also shown that due to a large difference in standard reduction potentials the silver and copper ions can be "kinetically" separated within both the hydrogenation and the oxygenation steps of the proposed process.

The important potential advantages of the proposed technique over the existing technologies for silver ions recovery are listed further. (1) The process is operated at ambient temperature and H_2&air gauge pressure of 1 bar. (2) It consumes only H_2 gas, air, and water (to compensate the electrochemical H_2O splitting). (3) The technique is highly selective for silver recovery, and the selectivity can be tuned by the pH within the H_2 and/or air steps of the process. (4) The process is highly effective for the recovery of Ag^{+} ions from dilute solutions. This is due to a high surface area of Pt/AC catalytic porous medium. (5) The process does not generate any secondary wastes. (6) The cost of the H_2 gas consumed by the process is expected to be very low compared to the cost of the recovered silver. For example, assuming a H_2 utilization efficiency of 30%, and the costs of electrolytic H_2 and silver of 6 US$/kg and 820 US$/kg (respectively), the cost of H_2 consumed by the process becomes only 0.022% of the recovered silver metal. (7) The process of Ag leaching followed by catalytic extraction and electrodeposition is balanced in respect of H^{+} ions and requires minimal addition (if any) of bases and/or acids.

In our future studies we will be focused on the investigation of the mechanisms involved in hydrogenation and oxygenation steps of the technology and on the development of mechanistic models that describe the kinetics of these two processes. Further studies are required also to optimize the utilization of Pt catalyst to minimize the capital costs of the process. The activated carbon applied in the present study as a support for Pt catalysts can be fouled due to adsorption of organic compounds. This phenomenon must be investigated, and appropriate reactivation methods developed to increase the operational life of the Pt/AC catalyst. The process must be also studied with other Pt catalyst carriers, such as alumina and titania.

CRediT authorship contribution statement

Erez B. Ruck: Investigation, Formal analysis, Methodology, Validation. **Gidon Amikam:** Methodology, Investigation. **Yonatan Darom:**

Methodology, Investigation. **Naama Manor-Korin:** Methodology, Investigation. **Youri Gendel:** Conceptualization, Supervision, Investigation, Methodology, Data curation, Funding acquisition, Project administration.

Declaration of Competing Interest

The authors declare that they have no known competing financial interests or personal relationships that could have appeared to influence the work reported in this paper.

Acknowledgements

This work was supported by the Israel Innovation Authority [KAMIN program, file number 75019].

References

[1] M.D. Rao, K.K. Singh, C.A. Morrison, J.B. Love, Challenges and opportunities in the recovery of gold from electronic waste, RSC Adv. 10 (8) (2020) 4300–4309, https://doi.org/10.1039/C9RA07607G.
[2] V. Forti, C.P. Baldé, R. Kuehr, G. Bel, The Global E-Waste Monitor 2020: Quantities, Flows, and the Circular Economy Potential; United Nations University: Tokyo, Japan, 2020; ISBN 9789280891140.
[3] G. Mishra, R. Jha, M.D. Rao, A. Meshram, K.K. Singh, Recovery of silver from waste printed circuit boards (WPCBs) through hydrometallurgical route: a review, Environ. Challenges 4 (2021) 100073, https://doi.org/10.1016/j.envc.2021.100073.
[4] M.S. Sodhi, B. Reimer, Models for recycling electronics and-of-life products, OR Spectrum 23 (2001) 97–115, https://doi.org/10.1007/PL00013347.
[5] M.A. Khaliq, G. Rhamdhani, S. Brooks, Masood, Metal extraction process for electronic waste and existing industrial routes: a review and Australian perspective, Resources 3 (2014) 152–179, https://doi.org/10.3390/resources3010152.
[6] S.M. Abdelbasir, S.S.M. Hassan, A.H. Kamel, R.S. El-Nasr, Status of electronic waste recycling techniques: a review, Environ. Sci. Pollut. Res. 25 (17) (2018) 16533–16547, https://doi.org/10.1007/s11356-018-2136-6.
[7] J. Cui, L. Zhang, Metallurgical recovery of metals from electronic waste: a review, J. Hazard. Mater. 158 (2-3) (2008) 228–256, https://doi.org/10.1016/j.jhazmat.2008.02.001.
[8] S. Syed, Recovery of gold from secondary sources—a review, Hydrometallurgy 115 (2012) 30–51, https://doi.org/10.1016/j.hydromet.2011.12.012.
[9] M. Kaya, Recovery of metals and nonmetals from electronic waste by physical and chemical recycling processes, Waste Manage. 57 (2016) 64–90, https://doi.org/10.1016/j.wasman.2016.08.004.
[10] A.K. Awasthi, M. Hasan, Y.K. Mishra, A.K. Pandey, B.N. Tiwary, R.C. Kuhad, V. K. Gupta, V.K. Thakur, Environmentally sound system for E-waste: biotechnological perspectives, Curr. Res. Biotechnol. 1 (2019) 58–64, https://doi.org/10.1016/j.crbiot.2019.10.002.
[11] U. Jadhav, H. Hocheng, Hydrometallurgical recovery of metals from large printed circuit board pieces, Sci. Rep. 5 (2015) 14574, https://doi.org/10.1038/srep14574.
[12] G.M. Ritcey, Solvent extraction in hydrometallurgy: present and future, Tsinghua Sci. Technol. 11 (2) (2006) 137–152, https://doi.org/10.1016/S1007-0214(06)70168-7.
[13] B. Robotin, A. Ispas, V. Coman, A. Bund, P. Ilea, Nickel recovery from electronic waste II Electrodeposition of Ni and Ni-Fe alloys from dilute sulfate solutions, Waste Manage. 33 (2013) 2381–2389, https://doi.org/10.1016/j.wasman.2013.06.001.
[14] T. Li, Z. Duan, R. Qin, X. Xu, B. Li, Y. Liu, M. Jiang, F. Zhan, Y. He, Enhanced characteristics and mechanism of Cu(II) removal from aqueous solutions in electrocatalytic internal micro-electrolysis fluidized-bed, Chemosphere 250 (2020) 126225, https://doi.org/10.1016/j.chemosphere.2020.126225.
[15] R. Martins, P.H. Britto-Costa, L.A.M. Ruotolo, Removal of toxic metals from aqueous effluents by electrodeposition in a spouted bed electrochemical reactor, Environ. Technol. 33 (10) (2012) 1123–1131, https://doi.org/10.1080/09593330.2011.610361.
[16] Z. Wang, P. Halli, P. Hannula, F. Liu, B.P. Wilson, K. Yliniemi, M. Lundström, Recovery of silver from dilute effluents via electrodeposition and redox replacement, J. Electrochem. Soc. 166 (8) (2019) E266–E274.
[17] Z. Wang, C. Peng, K. Yliniemi, M. Lundström, Recovery of high-purity silver from spent silver oxide batteries by sulfuric acid leaching and electrowinning, ACS Sustain. Chem. Eng. 8 (41) (2020) 15573–15583, https://doi.org/10.1021/acssuschemeng.0c04701.
[18] W. Sanchez-Ortiz, J. Aldana-Gonzalez, T.L. Manh, M. Romero-Romo, I. Mejia-Caballero, M.T. Ramirez-Silva, E.M. Arce-Estrada, V. Mugica-Alvarez, M. Palomar-Pardave, A deep eutectic solvent as leaching agent and electrolytic bath for silver recovery from spent silver oxide batteries, J. Electrochem. Soc. 168 (2021) 016508.
[19] A. Imre-Lucaci, M. Fogarasi, F. Imre-Lucaci, S. Fogarasi, Chemical-electrochemical process concept for lead recovery from waste cathode ray tube glass, Materials 14 (2014) 1546, https://doi.org/10.3390/ma14061546.
[20] Y. Jian-guang, L. Jie, P. Si-yao, L. Yuan-lu, S. Wei-qiang, A new membrane electrodeposition based process for tin recovery from waste printed circuit boards, J. Hazard. Mater. 304 (2016) 409–416, https://doi.org/10.1016/j.jhazmat.2015.11.007.
[21] M. Lekka, I. Masavetas, A.V. Benedetti, A. Moutsatsou, L. Fedrizzi, Gold recovery from waste electrical and electronic equipment by electrodeposition: a feasibility study, Hydrometallurgy 157 (2015) 97–106, https://doi.org/10.1016/j.hydromet.2015.07.017.
[22] P.H. Britto-Costa, L.A.M. Ruotolo, Mass transfer study on the electrochemical removal of copper ions from synthetic effluents using reticulated vitreous carbon, Environ. Technol. 34 (4) (2013) 437–444, https://doi.org/10.1080/09593330.2012.698651.
[23] L.A.M. Ruotolo, J.C. Gubulin, Electrodeposition of copper ions on fixed bed electrodes: kinetics and hydrodynamic study, Braz. J. Chem. Eng. 19 (1) (2002) 105–118, https://doi.org/10.1590/S0104-66322002000100008.
[24] B.J. Sabacky, J.W. Evans, Electrodeposition of metals in fluidized-bed electrodes. 2. Experimental investigation of copper electrodeposition at high-current density, Journal of the Electrochemical Society 126(7) (1979) 1180-1187. https://doi.org/10.1149/1.2129239.
[25] Y. Darom, G. Amikam, E.B. Ruck, Y. Gendel, Capacitive-faradaic fuel cells (CFFCs) for selective separation of copper (II) ions from water and wastewater, Chem. Eng. J. 421 (1) (2021) 129950, https://doi.org/10.1016/j.cej.2021.129950.
[26] M.A. Rizvi, R.M. Syed, B. Khan, Complexation effect on redox potential of iron(III)-Iron(II) couple: a simple potentiometric experiment, J. Chem. Educ. 88 (2) (2011) 220–222, https://doi.org/10.1021/ed100339g.
[27] A. Agrawal, V. Kumar, B.D. Pandey, K.K. Sahu, A comprehensive review on the hydro metallurgical process for the production of nickel and copper powders by hydrogen reduction, Mater. Res. Bull. 41 (4) (2006) 879–892, https://doi.org/10.1016/j.materresbull.2005.09.028.
[28] B.G. Ershov, E.V. Abkhalimov, Nucleation of silver upon the reduction by hydrogen in aqueous polyphosphate-containing solutions: formation of clusters and nanoparticles, Colloid J. 69 (5) (2007) 579–584, https://doi.org/10.1134/S1061933X07050079.
[29] K.J. Hartlieb, M. Saunders, R.J.J. Jachuck, C.L. Raston, Continuous flow synthesis of small silver nanoparticles involving hydrogen as a reducing agent, Green Chem. 6 (2010) 1012–1017, https://doi.org/10.1039/C000708K.
[30] G. Amikam, N. Manor-Korin, P. Nativ, Y. Gendel, Separation of ions from water and wastewater using micro-scale capacitive-faradaic fuel cells (CFFCs), powered by $H_{2(g)}$ and air, Sep. Purif. Technol. 253 (2020) 117494, https://doi.org/10.1016/j.seppur.2020.117494.
[31] G. Amikam, Y. Gendel, Separation and hydrogenation of nitrate ions by micro-scale capacitive-faradaic fuel cells (CFFCs), Electrochem. Commun. 120 (2020) 106831, https://doi.org/10.1016/j.elecom.2020.106831.
[32] M.H. Morcali, Recycling of silver and zinc from silver oxide battery waste, ChemistrySelect 4 (31) (2019) 9011–9017, https://doi.org/10.1002/slct.201900659.
[33] T. Wen, F. Qu, N.B. Li, H.Q. Luo, A facile, sensitive, and rapid spectrophotometric method for copper(II) ion detection in aqueous media using polyethyleneimine, Arabian J. Chem. 10 (2) (2017) S1680–S1685, https://doi.org/10.1016/j.arabjc.2013.06.013.
[34] Y. Jia, G.P. Demopoulus, Adsorption of silver onto activated carbon from acidic media: nitrate and sulfate media, Ind. Eng. Chem. Res. 42 (1) (2003) 72–79, https://doi.org/10.1021/ie020335k.
[35] A. Naumkin, Problems in determination of Ag charge state atoms in silver nanoparticles by X-Ray photoelectron spectroscopy, Scientific J. Biomed. Eng. Biomed. Sci. 2 (1) (2018) 014–016.
[36] C.J. Powell, Recommended Auger parameters for 42 elemental solids, J. Electron Spectrosc. Relat. Phenom. 185 (1–2) (2012) 1–3, https://doi.org/10.1016/j.elspec.2011.12.001.
[37] I.V. Artamonova, I.G. Gorichev, E.B. Godunov, Kinetics of manganese oxides dissolution in sulphuric acid solutions containing oxalic acid, Engineering 05 (09) (2013) 714–719, https://doi.org/10.4236/eng.2013.59085.
[38] E.B. Godunov, A.D. Izotov, I.G. Gorichev, Dissolution of manganese oxides of various compositions in sulphuric acid solutions studied by kinetic methods, Inorg. Mater. 54 (1) (2018) 66–71, https://doi.org/10.1134/S002016851801003X.